doi: 10.1111/j.1365-3121.2008.00798.x

High rate GPS data on active volcanoes: an application to the 2005–2006 Mt. Augustine (Alaska, USA) eruption

Mario Mattia,[1] Mimmo Palano,[1] Marco Aloisi,[1] Valentina Bruno[1,2] and Yehuda Bock[3]

[1]*Istituto Nazionale di Geofisica e Vulcanologia, sezione di Catania, P.zza Roma 2, Catania, Italy;* [2]*Dipartimento di Geologia e Geofisica, Università degli Studi di Catania, Corso Italia 55, Catania, Italy;* [3]*Cecil H. and Ida M. Green Institute of Geophysics and Planetary Physics, Scripps Institution of Oceanography, La Jolla, CA, USA*

ABSTRACT

Volcanic eruptions are usually preceded by measurable signals of growing unrest, the most evident of which are the increase in seismicity and ground deformation. It is also important to identify precursors of a possible renewal of the volcanic activity and to distinguish between an eruptive activity characterized by an intrusion (with the related destructive power) and a migration of magma stored in the main conduits. The 2005–2006 eruption at Mt. Augustine (Alaska, USA) is a good example of a massive migration of magmatic fluids from depth (about 1 km b.s.l.) under the effect of gas overpressure. The movements, recorded by High Rate GPS (HRGPS) data (15 s of sampling and processing rate) from the stations deployed on the volcano, define the dimensions and the characteristics of the shallow plumbing system. In this study, we propose a model of the different stages preceding the effusive phase (the 'precursory phase'), where gas overpressure in the body of the volcano opens the terminal conduit.

Terra Nova, 20, 134–140, 2008

Introduction

Augustine volcano is a 1260-m-high dacitic stratovolcano located in lower Cook Inlet region, about 280 km south-west of Anchorage, Alaska (Fig. 1). It consists of a central dome and lava flow complex, surrounded by pyroclastic debris (Miller *et al*., 1998). Prior to the 2006 eruption, Augustine volcano had six major historically reported eruptions (1812, 1883, 1935, 1963–64, 1976 and 1986) (Miller *et al*., 1998). Historical eruptions typically consisted of explosive activity with emplacement of pumiceous pyroclastic-flow deposits followed by lava dome extrusion with associated block-and-ash flows. Typical eruptions of Augustine volcano are capable of outpouring large volumes of volcanic ash that may rise to more than 12 km a.s.l. These clouds of volcanic ash are hazardous to jet aircraft in the Cook Inlet region and for thousands of kilometre downwind from the volcano. Furthermore, volcanic debris that fall or flow into the sea may initiate local wave phenomena (tsunamis) that may be hazardous to shipping or people close to Augustine volcano (less than about 5 km) (Waythomas and Waitt, 1998). The nature of volcano hazards at Augustine volcano implies the necessity to forecast timely warnings of volcanic unrest and potential eruptions. Transient episodes of ground displacement related to the dynamics of magmatic fluids as possible precursors to eruptive activity can be revealed through a careful analysis of High Rate GPS (HRGPS) data. In the first phases of an eruption, the real time processing of HRGPS data can be used by civil protection authorities to monitor the opening of fracture fields on the slopes of volcanoes under the pressure of gas and magma. During eruption, large explosions, opening of vents, migration of fractures fields, landslides and other dangerous phenomena can be monitored and their potential for damage estimated. This technique was previously applied to model the 2002–2003 Stromboli Island (Italy) eruption (Mattia *et al*., 2004).

In this work, we have processed the GPS data of the stations on Augustine volcano (Fig. 1) spanning from September 2005 to January 2006 and recorded by five continuously recording GPS instruments, installed in the framework of the Earthscope project by the National Science Foundation's Plate Boundary Observatory (PBO). In particular, the entire dataset was processed in the first step, by using the GAMIT/GLOBK software packages (Herring, 2000; King and Bock, 2004) and in the second step, by applying the method of instantaneous GPS positioning (Bock *et al*., 2000). Both daily and 15-min coordinate time series show clear evidence of the dynamics leading to the 2005–2006 eruption; then, the main signals are modelled to reveal new insights on the intrusion processes acting before and during the eruption of Augustine volcano.

It is important to underline that other authors (Cervelli *et al*., 2006) have modelled the same GPS data to image the source of the 2005–2006 Mt. Augustine eruption. These authors have found that a simple Mogi source can explain the cumulative deformation preceding the eruptive phase (from May 2005 to 17 November 2005). We improve on the analysis of Cervelli *et al*. (2006) following their suggestion of a more complex source mechanism for the pre-eruptive phase, improving the final results mainly for the vertical deformation. We also find that there are several other stages with respect to three (Early Precursory, Late Precursory and Early Eruptive, respectively) stages suggested by Cervelli *et al*. (2006) testifying to a more complex pattern of dike propagation.

Chronology of the 2006 eruptive event

The 2006 Augustine volcano eruption was heralded by a steady increase in microearthquakes beneath the volcano in May 2005 (Cervelli *et al*., 2006). Deformation began in early

Correspondence: M. Mattia, Istituto Nazionale di Geofisica e Vulcanologia, Sezione di Catania, P.zza Roma, 2, 95123 Catania, Italy. Tel.: +39 95 7165805; fax: +39 95 435801; e-mail: mattia@ct.ingv.it

summer 2005 coupled with small gas emission. On 17 November 2005, the seismic rate increase drastically; over the next day (2 December 2005), seismometers began recording signals from small phreatic explosions, although the largest signals began on December 10 (Fig. 1). An overflight on 12 December 2005 revealed vigorous venting of steam and gas from the summit and a dusting of ash on the south and south-east flanks of the volcano (Power *et al*., 2006). After a period of phreatic explosions and vigorous degassing, on early 11 January 2006, an energetic swarm of volcano-tectonic earthquakes began, culminating in two large explosions on the same day, which produced ash plumes with heights exceeding 9 km a.s.l. On 13 January 2006, six juvenile-rich powerful explosions began, preceded by an increasing seismicity, which continued throughout the sequence. GPS station AV05 was destroyed by the first of these explosions. An explosive eruption on 17 January 2006 generated a column higher than 13 km a.s.l. Data transmission from station AV04 stopped in coincidence with this event. The eruption of 13–17 January generated pumiceous pyroclastic flows, snow avalanches and lahars that moved down the volcano's flanks (Power *et al*., 2006). In the following days, no explosion occurred, and seismicity diminished considerably. Renewed explosive activity, again preceded by increasing seismicity, began on January 28, 2006 with an event that raised ash up to 9 km a.s.l. Station AV03 was destroyed during this event. In the following days, seven additional explosions occurred and the activity evolved into nearly continuous effusion and dome building.

Data processing

GPS data were processed adopting two different strategies. In the first approach, the data were processed using the GAMIT/GLOBK software packages (Herring, 2000; King and Bock, 2004). To improve the overall configuration of the network and to combine the individual solutions in GLOBK, data from five continuously operating IGS stations (AC59, FAIR, WHIT, KOD1 and ATW2; Fig. 1) were also included in the processing. The basic products of the processing were GAMIT 'h-files', loosely-constrained solutions containing a set of one-day site estimate positions, Earth orientation parameters and associated error covariance matrices. Next, the individual 'h-files' were combined, on a daily basis, using the GLOBK Kalman filter with regional (IGS1, IGS2, IGS3, IGS4 and AKDA) solutions provided by the SOPAC (Scripps Orbit and Permanent Array Center – ftp://garner.ucsd.edu/pub/hfiles), to create a daily unconstrained combined network solution. The loosely constrained daily solutions were transformed into the ITRF2000 Reference frame (Altamimi *et al*., 2002) by means of an Helmert transformation using the GLORG module of GLOBK (Herring, 2000). Finally, we estimated the 24-h NEU-component time series for stations AV01, AV02, AV03 AV04 and AV05 (Fig 1). The RMS scatter of the daily time series prior to the onset of volcanic deformation is 2.3–3.1 mm in the horizontal and 5.5–7.8 mm in the vertical component.

To improve temporal resolution during periods of deformation, the data were processed in a second approach by applying the method of instantaneous GPS positioning (Bock *et al*., 2000), successfully applied to volcano monitoring (Mattia *et al*., 2004). Instantaneous positioning provides independent relative position estimates, at each observation epoch, by resolving integer-cycle phase ambiguities anew for each epoch. This approach provides advantages over static and real-time kinematic methods or related post-processed filtering methods, which require multiple epochs to resolve phase ambiguities and to maintain phase continuity in the presence of communications outages, losses of receiver lock, and sub-optimal satellite visibility, often experienced on the steep flanks of active volcanoes. We used the Geodetics RTD software package to analyse the 15 s GPS data. The instantaneous positions of the volcano stations were computed relative to station AC59, at a distance of about 25 km. The station coordinates were unconstrained and for this preliminary analysis, we did not make use of the *a priori* daily coordinates available from the GAMIT/GLOBK analysis. RTD produced 15-min median values from the 15-s instantaneous positions. The RMS scatter of the 15-min time series prior to the onset of volcanic deformation is 2.0–3.2 mm in the horizontal and 5.0–18.0 in the vertical component. We applied a cleaning algorithm to reduce the amount of outliers in the 15-min position time series because of uncertain estimates of integer ambiguities and other errors. For example, the summit stations AV04 and AV05 clearly show an increasing noise in November 2005 that may be related to snow accumulation on the GPS antenna (Cervelli *et al*., 2006) (Fig. 1). In particular, for each site and for each coordinate, outliers are defined as having:

$$\left|p_i - \bar{p}_{i-w/2,i+w/2}\right| > \sigma_{i-w/2,i+w/2}$$

where p is the measurement; $\bar{p}$ is the average value computed within a sliding window of size w centred on each measurement and σ is the standard deviation computed also within the sliding window. In addition, we assumed that σ did not exceed 5 cm, in agreement with the maximum observed variation of the daily solution. With this criterion, the filter removed 20–45% of the data from each site. Percentages are computed with respect to the number of available data.

Both daily and 15-min coordinate time series show clear evidence of the dynamics leading to the 2006 eruption (Fig. 1). In the following, the results are analysed and modelled to understand the main processes acting before the eruption onset of Augustine volcano.

Data analyses and inversions

Daily and 15-min coordinate time series at AV04 and AV05 are reported in Fig. 1. The slope changes at each NEU site coordinates allowed us to detect at least eight different stages (Fig. 1). We have reported in Fig. 2 the displacement vectors for each slope change in the GPS stations time series.

To model the observed displacements at Augustine during each stage, we inverted the ground deformations assuming simple dislocations (Okada, 1985) by adopting a least-squares (Tarantola and Vallette, 1982) method, or a point-pressurized cavity of ellipsoidal shape (Davis, 1986) by

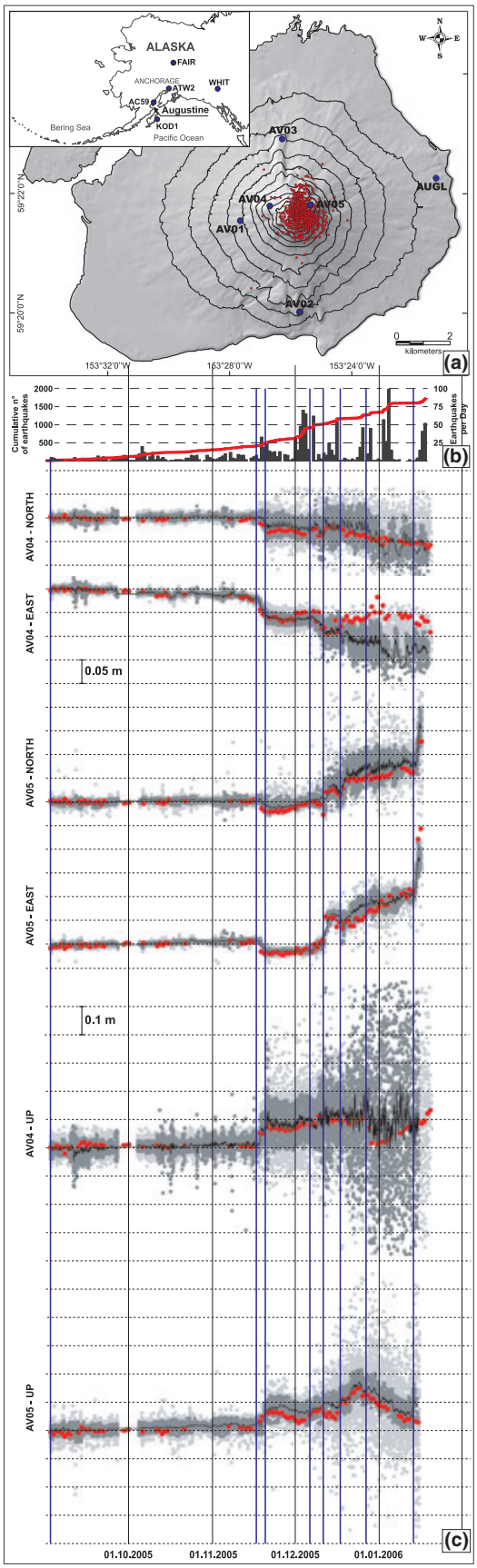

adopting a genetic algorithm (e.g. Nunnari *et al.*, 2005). In this step, both horizontal and vertical GPS components were inverted. Values of 30 GPa and 0.25, respectively, for the shear modulus and Poisson's ratio were assumed in the inversion. The rigidity chosen represents an averaged value for crustal rigidity of volcanic areas (e.g. Williams and Wadge, 2000; Trasatti *et al.*, 2003). The parameters used as 'starting points' for the inversion procedure are listed in Table 1. We inverted stages 1, 3, 4, 6 and 7 because stages 2, 5 and 8 showed inelastic behaviour of the upper pattern of the volcano edifice, discouraging any attempt to invert the data by adopting classical volcanic source models. In particular, we adopted a Davis-type source for stage 1 and Okada-type sources for stages 3, 4, 6 and 7. The best source parameters resulting for each inverted stage, referred to a system defined according to the local UTM coordinates, are summarized in Table 2. The reference surface was assumed at the medium height of the GPS stations (0.6 km a.s.l.). The source parameter error was calculated as the standard deviation in the class of all the solutions that satisfy the chi-squared test for our degrees of freedom within the significance level of 5% (Table 2). Considering the results of the inversions, each model is able to explain, within the error, the observed pattern of ground deformation. Moreover, considering the source parameter error values (Table 1), the Okada-type sources inferred for stages 3, 4, 6 and 7 coincide within the errors, with a unique source. The small differences in positions could be related to noise within the data. Starting from the results obtained for stage 3, a new inversion for stages 4, 6 and 7 was performed. In particular, the positions and dimensions of the Okada-type sources were fixed to those found for stage 3, inverting only its dip, strike motion and opening. The best source parameters resulting for each stage are summarized in Table 3.

Discussions and conclusions

The HRGPS analysis applied to the 2006 Mt. Augustine volcano eruption allowed us to detect the timing of, at least, eight different stages in the

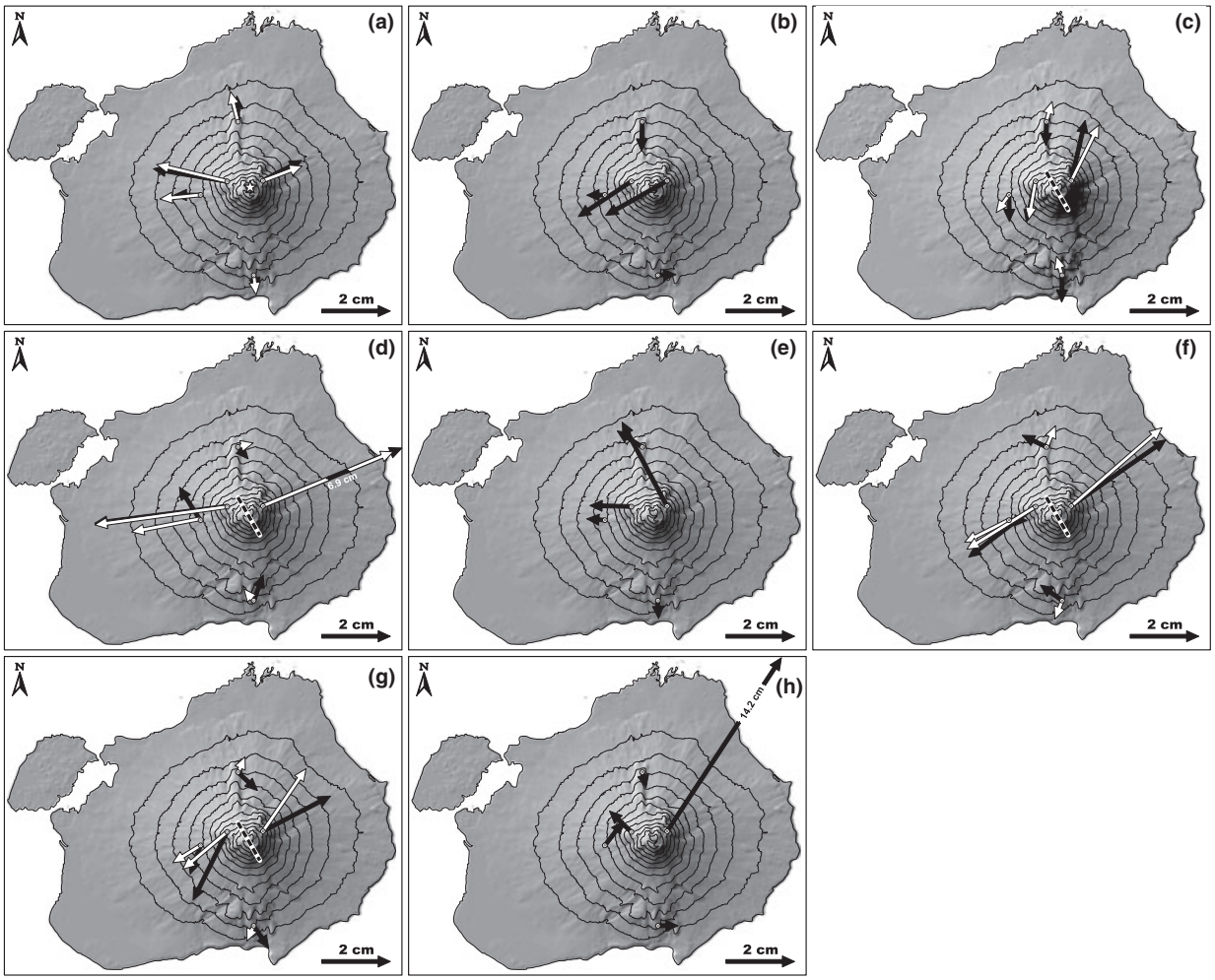

Fig. 2 Comparison between observed (black arrows) and expected (white arrows) horizontal displacements relevant to each stage: (a) 03.09.05–16.11.05; (b) 16.11.05–20.11.05; (c) 20.11.05–06.12.05; (d) 06.12.05–10.12.05; (e) 10.12.05–16.12.05; (f) 16.12.05–23.12.05; (g) 23.12.05–11.01.06; (h) after 11.01.06. Modelled sources are also reported.

Fig. 1 (a) Shaded relief map of Augustine volcano showing locations of GPS stations (blue points). Earthquake locations (red points), occurred during September 2005 to January 2006 time interval are also reported. In the inset, locations of AC59, FAIR, WHIT, KOD1 and ATW2 stations are also reported (see text for details). (b) Temporal histogram of located earthquakes. The red line indicates the cumulative number of located earthquakes (redrawn from Cervelli *et al*., 2006). (c) Daily and 15-min time series of N, E and U coordinates at AV04 and AV05. The daily solution obtained by using the GAMIT/GLOBK software packages are reported in red; the 15-min solutions obtained by the Geodetics RTD software package are reported both as un-filtered (light-grey) and filtered (dark-grey) time series (see text for details). In black, the weighted average for each filtered time series is also reported. The blue vertical lines marked the division of the time series into different stages. The *y*-values of U coordinates were clipped at −0.38 and 0.58. Since 3 September 2005, the time-position of each GPS station showed a linear deformation rate until 19:22 hours on 16 November 2005 (stage 1) (all times UTC), when a marked change in deformation rate was observed at AV04 and AV05 HRGPS time series. This event was accompanied in the following hours by an increase in the seismicity (Cervelli *et al*., 2006) (stage 2). After 11:07 hours on 20 November, the deformation rate strongly decreased showing a linear trend until 00:52 hours on 6 December (stage 3). In the following days, a new change in deformation rate was observed at AV04 and AV05 stations, indicating a clear intrusive episode (stage 4). Since 2 December, seismometers began recording signals from small phreatic explosions, although the largest signals began on December 9 (Cervelli *et al*., 2006) with the occurrence at 20.07 hours of an abrupt change in deformation rate at station AV05 (AV04 showed a small offset) (stage 5). An intrusive episode started in late afternoon of 16 December (stage 6). This period was characterized by the occurrence of phreatic explosions and vigorous degassing and was accompanied by the opening of fissures at the summit area (Cervelli *et al*., 2006). At 04:52 hours on 23 December, a decrease in the deformation rate in the horizontal component of AV04 and AV05 was observed; moreover, a marked change on the rate (from uplift to subsidence) of the Up component at AV05 was observed (stage 7). At 01:15 hours on 11 January 2006, a strong seismic swarm began, culminating in two large explosions at 13:44 and 14:12 hours (stage 8). On 13 January, another six large explosions began, preceded by an increasing seismicity, which continued throughout the sequence. Station AV05 was destroyed by the first of these explosions.

Table 1 'Starting value' (LS approach) and 'range search' (GA approach) for the parameters of the adopted source models. Coordinates are WGS84–UTM 5N.

	Davis-type source		Okada-type source
	Range search		
	Min	Max	Starting values
Longitude (km)	470.00	480.00	475.00
Latitude (km)	6575.00	6585.00	6580.00
Azimuth			N150°E*
Depth (km)	1.00 b.s.l.	6.00 a.s.l.	0.00 a.s.l.
Length (km)			0.5
Width (km)			0.5
Dip			89.9
Strike-slip (cm)			0.0
Dip-slip (cm)			0.0
Opening (cm)			0.0
$P \times V^3$ (Pa × m^3)	$-5.00 \cdot 10^{17}$	$5.00 \cdot 10^{17}$	
1^ Euler angle	−180°	180°	
2^ Euler angle	−180°	180°	
3^ Euler angle	−180°	180°	
b/a	0.10	0.99	
c/a	0.10	0.99	

unrest state of this volcano. The ground deformation pattern for each stage, was inverted by adopting classical elastic deformation models (e.g. Okada, 1985; Davis, 1986), assuming that the volcano behaves as a homogeneous, isotropic, elastic semi-infinite plate. Several studies (De Natale and Pingue, 1993; Trasatti *et al*., 2003; Gudmundsson and Brenner, 2004a,b, 2005; Gudmundsson, 2006) showed that mechanical layering, contacts, faults and fractures affect the measured surface deformation associated with dike propagation or magma chamber inflation or deflation during an unrest period. However, by making the models more complex, even if the fit would be improved, there is a serious risk of 'modelling' noise.

For stage 1, we inferred a source, located at approximately sea level (about 0.33 km b.s.l.) (Fig. 3) with a vertically elongated shape. The position of this source is very close to that obtained by Cervelli *et al*., 2006. It is remarkable that, for this stage, the misfit of the vertical deformations is very low compared with the results of the Mogi-type (Mogi, 1958) source found by Cervelli *et al*. (2006), testifying that a geometrically more complex source than a point source worked in the early precursory stage. For stages 3, 4, 6 and 7, in a first step, we obtained four distinct dike-shaped sources. However, considering the error in the estimate of the sources, we can assume that a unique 'intrusive volume' has produced the observed pattern of ground deformation. The small differences in positions could be related to noise within the data. A new inversion was performed fixing positions and dimensions of the source to the results obtained for stage 3 inverting only its dip-, strike-motion and opening (Fig. 3). The ground deformation observed in stages 2, 5 and 8 indicated inelastic behaviour of the upper part of the volcano, discouraging any attempt to invert the data. This fact supports the idea that the different mechanisms of every single stage of the pre-eruptive phase are related to different velocities of upward transport (or flow) of fluids. In particular, when the variations are faster, the behaviour of the medium is brittle and the pattern of ground displacement is not modellable.

Another key conclusion from this analysis is the very low amount of volumetric variations associated with the 'precursory stage' of the 2006 eruption. In our opinion, this is

Table 2 Parameters of the modelled sources inferred for each stage. Coordinates are WGS84–UTM 5N. The azimuth of the Okada-type source was fixed according the striking of the fissures opened at the summit area (Cervelli *et al*., 2006).

	Stage 1	Stage 3	Stage 4	Stage 6	Stage 7
	03.09.05–16.11.05	20.11.05–06.12.05	06.12.05–10.12.05	16.12.05–23.12.05	23.12.05–11.01.06
Longitude (km)	475.54	475.48 ± 0.31	475.34 ± 0.25	475.32 ± 0.33	475.21 ± 0.35
Latitude (km)	6580.03	6580.18 ± 0.34	6580.09 ± 0.34	6580.34 ± 0.36	6580.23 ± 0.36
Azimuth		N150°E	N150°E	N150°E	N150°E
Depth (km)	0.30 b.s.l.	0.60 ± 0.36 a.s.l.	0.60 ± 0.19 a.s.l.	0.45 ± 0.35 a.s.l.	0.60 ± 0.36 a.s.l.
Length (km)		1.5 ± 0.32	1.4 ± 0.31	0.8 ± 0.34	1.0 ± 0.35
Width (km)		0.9 ± 0.35	0.9 ± 0.33	0.4 ± 0.33	0.6 ± 0.36
Dip		81° ± 11.1°	77° ± 13.7°	76° ± 14.1°	78° ± 14.1°
Strike-slip (cm)		7.3 ± 6.2	−11 ± 6.9	35 ± 7.1	9 ± 7.0
Dip-slip (cm)		−0.9 ± 6.5	19.1 ± 7.0	0.6 ± 7.1	3 ± 7.0
Opening (cm)		4.8 ± 5.6	15.3 ± 6.6	44 ± 7.1	12 ± 7.0
$P \times V^3$ (Pa × m^3)	$5.69 \cdot 10^{15}$				
1^ Euler angle	−72.1°				
2^ Euler angle	58.6°				
3^ Euler angle	59.8°				
b/a	0.47				
c/a	0.34				
ΔV (m^3)	2.16×10^5	$6.48 \pm 8.1 \times 10^4$	$1.93 \pm 1.2 \times 10^5$	$1.41 \pm 1.3 \times 10^5$	$7.20 \pm 6.5 \cdot 10^4$

Table 3 Parameters of the modelled sources inferred for each stage. Coordinates are WGS84–UTM 5N.

	Stage 4	Stage 6	Stage 7
	06.12.05–10.12.05	**16.12.05–23.12.05**	**23.12.05–11.01.06**
Longitude (km)	475.48*	475.48*	475.48*
Latitude (km)	6580.18*	6580.18*	6580.18*
Azimuth	N150°E*	N150°E*	N150°E*
Depth (km)	0.60*	0.60*	0.60*
Length (km)	1.5*	1.5*	1.5*
Width (km)	0.9*	0.9*	0.9*
Dip	81°*	81°*	81°*
Strike-slip (cm)	−7.5 ± 6.3	5.3 ± 6.3	7.2 ± 6.3
Dip-slip (cm)	11.3 ± 6.2	1.5 ± 6.4	−3.2 ± 6.3
Opening (cm)	14.3 ± 6.0	11.2 ± 6.2	7.2 ± 6.1
$P \times V^3$ (Pa × m^3)			
1^ Euler angle			
2^ Euler angle			
3^ Euler angle			
b/a			
c/a			
ΔV (m^3)	1.9 ± 1.2 × 10^5	1.5 ± 1.1 × 10^5	1.0 ± 0.9 × 10^5

*Fixed values to results obtained for stage 3 (see Table 2).

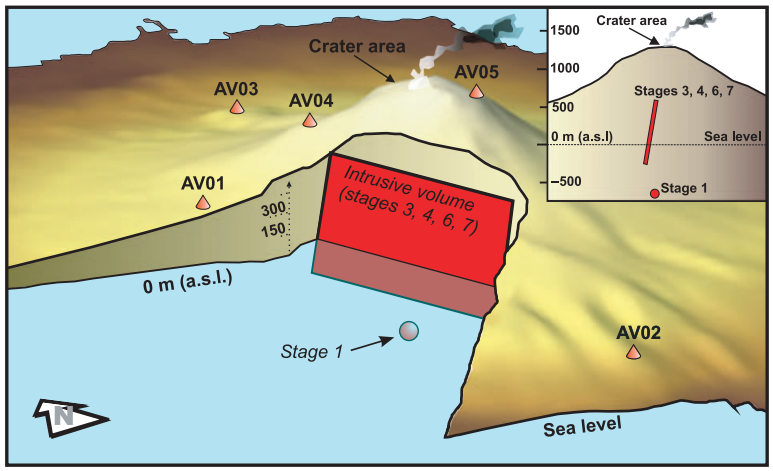

Fig. 3 Three-dimensional model sketch. GPS stations are also shown. A schematic N60°E–N120°W-oriented cross-section showing the geometrical relationships between the sources modelled in this work is shown in the inset. Davis model dimensions are strictly indicative.

strictly related to the prevailing action of gas in opening the conduit of Mt. Augustine. Following this hypothesis, the shallow plumbing system of the volcano pressurized (probably under the pushing action of a juvenile magma batch) the main conduit (dike-shaped) creating the conditions for the eventual uprise of juvenile magma. In fact, as reported by preliminary petrographic analysis (Izbekov *et al.*, 2006), the first explosive phase of juvenile material can be dated to 13 January 2006. Moreover, until the explosive phase of mid January, the explosions where mainly phreatic with old remobilized tephra involved, testifying to a phase where the action of gas was prevailing.

Finally, we want to underline the importance that real time data processing has in volcano monitoring. In fact, one of the major concerns of the eruptive activity of Augustine is related to the interaction of the volcanic ash erupted and the flights of civil and military airplanes. As demonstrated in this work, every change (also small) in the shape of the volcano during a period of unrest can be related to a variation in the position of magmatic fluids in the body of the volcano itself. As a results of this physical change, the possibility of large explosions increases. Furthermore, if we assume that an increased seismicity, marked variations in continuously monitored geochemical parameters, and sudden changes in other geophysical parameters (magnetic field, gravity, etc.) can alert an Observatory to the impending possibility of an eruption, only the high rate monitoring of ground deformation can help define where the episode of unrest is occurring. This aspect is fundamental to a volcano like Augustine where, in the past (Waythomas and Waitt, 1998), tsunamigenic volcanic flows occurred.

Acknowledgements

The authors thank two anonymous reviewers for their constructive suggestions, and the Associate Editor, August Gudmundsson, for his helpful comments. We are also grateful to Francesco Guglielmino and Flavio Cannavò for the GA code used in the inversion process. We also acknowledge the National Science Foundation's Earthscope project, the Plate Boundary Observatory, and UNAVCO Inc. for the GPS data.

References

Altamimi, Z., Sillard, P. and Boucher, C., 2002. ITRF2000: A new release of the International Terrestrial Reference Frame for earth science applications. *J. Geophys. Res.*, **107**, 2214, doi: 10.1029/2001JB000561.

Bock, Y., Nikolaidis, R., de Jonge, P.J. and Bevis, M., 2000. Instantaneous resolution of crustal motion at medium distances with Global Positioning System. *J. Geophys. Res.*, **105**, 28.223–28.254.

Cervelli, P.F., Fournier, T., Freymueller, J. and Power, J.A., 2006. Ground deformation associated with the precursory unrest and early phases of the January 2006 eruption of Augustine Volcano, Alaska. *Geophys. Res. Lett.*, **33**, doi: 10.1029/2006GL027219.

Davis, P.M., 1986. Surface deformation due to inflation of an arbitrarily oriented triaxial ellipsoidal cavity in an elastic half-space, with reference to Kilauea volcano, Hawaii. *J. Geophys. Res.*, **91**, 7429–7438.

De Natale, G. and Pingue, F., 1993. Ground deformation in collapsed calderas structures. *J. Volcanol. Geotherm. Res.*, **57**, 19–38.

Gudmundsson, A., 2006. How local stresses control magma-chamber ruptures, dyke injections, and eruptions in composite volcanoes. *Earth Sci. Rev.*, **79**, 1–31. doi: 10.1016/j.earscirev.2006.06.006.

Gudmundsson, A. and Brenner, S.L., 2004a. How mechanical layering affects local stresses, unrests, and eruptions of volcanoes. *Geophys. Res. Lett.*, **31**. doi: 10.1029/2004GL020083.

Gudmundsson, A. and Brenner, S.L., 2004b. Local stresses, dyke arrest and surface deformation in volcanic edifices and rift zones. *Ann. Geophys.*, **47**, 1433–1454.

Gudmundsson, A. and Brenner, S.L., 2005. On the conditions of sheet injections and eruptions in stratovolcanoes. *Bull. Volcanol.*, **67**, 768–782.

Herring, T., 2000. *Global Kalman Filter VLBI and GPS Analysis Program*, Version 5.0. Massachusetts Institute of Technology, Cambridge, MA.

Izbekov, P., Wallace, K., Larsen, J., Nye, C. and Eichelberger, J., 2006. Variations of glass composition at the start of the 2006 eruption, Augustine volcano, Alaska. *Geol. Soc. Am. Abstr. Programs*, **38**, 76.

King, R. and Bock, Y., 2004. *Documentation for the GAMIT GPS Analysis Software, Release 10.2*. Massachusetts Institute of Technology, Cambridge, MA, and Scripps Institute of Oceanography, La Jolla, CA.

Mattia, M., Rossi, M., Guglielmino, F., Aloisi, M. and Bock, Y., 2004. The shallow plumbing system of Stromboli Islands imaged from 1 Hz instantaneous GPS positions. *Geophys. Res. Lett.*, **31**, L24610, doi: 10.1029/2004GL021281.

Miller, T.P., McGimsey, R.G., Richter, D.H., Riehle, J.R., Nye, C.J., Yount, M.E. and Dumoulin, J.A., 1998. Catalog of the historically active volcanoes of Alaska. *U.S. Geol. Surv. Open-File Rep.*, **98**, 104.

Mogi, K., 1958. Relation between the eruptions of various volcanoes and the deformations of the ground surfaces around them. *Bull. Earth Res. Inst.*, **36**, 99–134.

Nunnari, G., Puglisi, G. and Guglielmino, F., 2005. Inversion of SAR data in active volcanic areas by optimization techniques. *Nonlinear Process. Geophys.*, **12**, 1–8.

Okada, Y., 1985. Surface deformation due to shear and tensile fault in half-space. *Bull. Seismol. Soc. Am.*, **75**, 1135–1154.

Power, J.A., Nye, C.J., Coombs, M.L., Wessels, R.L., Cervelli, P.F., Dehn, J., Wallace, K.L., Freymueller, J.T. and Doukas, M.P., 2006. The reawakening of Alaska's Augustine Volcano. *EOS*, **87**, 373–377.

Tarantola, A. and Vallette, B., 1982. Generalized nonlinear inverse problems solved using the least squares criterion. *Rev. Geophys. Space Phys.*, **20**, 219–232.

Trasatti, E., Giunchi, C. and Bonafede, M., 2003. Effects of topography and rheological layering on ground deformation in volcanic regions. *J. Volcanol. Geotherm. Res.*, **122**, 89–110.

Waythomas, C.F. and Waitt, R.B., 1998. Preliminary volcano-hazard assessment for Augustine Volcano, Alaska. *U.S. Geol. Surv. Open-File Rep.*, **98–106**, 46 pp.

Williams, C.A. and Wadge, G., 2000. An accurate and efficient method for including the effects of topography in three-dimensional elastic models of ground deformation with applications to radar interferometry. *J. Geophys. Res.*, **105**, 8103–8120.

Received 8 June 2007; revised version accepted 18 January 2008

